



ChemComm

Isomerizations of a Pt₄ Cluster Revealed by Spatiotemporal Microscopic Analysis

Journal:	<i>ChemComm</i>
Manuscript ID	CC-COM-01-2019-000530.R2
Article Type:	Communication

SCHOLARONE™
Manuscripts



Journal Name

COMMUNICATION

Isomerizations of a Pt₄ Cluster Revealed by Spatiotemporal Microscopic Analysis

Takane Imaoka,^{*a,b,c} Tetsuya Toyonaga,^a Mari Morita,^b Naoki Haruta^b and Kimihisa Yamamoto^{*a,b}

Received 00th January 20xx,
Accepted 00th January 20xx

DOI: 10.1039/x0xx00000x

www.rsc.org/

We now report the first direct observation of the fluxional nature in which the four-atomic platinum cluster (Pt₄) randomly walks through several isomers. Time-lapse analysis by a Cs-corrected transmission electron microscope allowed us to acquire the atomic coordinates at a sub-angstrom space resolution and 0.2 s time resolution for each cluster isomer. The analysis revealed that the isomerization follows a simple first-order kinetic model.

Metal clusters and ultrasmall nanoparticles expected as promising catalysts^{1–7} are nanomaterials which consist of a myriad of compositions and the combinations of the constituent atoms. In addition to the compositional variation, recent computational studies of metal clusters proposed the importance of fluxionality,^{8–10} which means that the structure of the cluster changes from moment to moment with fluctuation. The fluxionality is a key principle to understand enzymatic catalysts.^{11,12} However, this point of view makes it more difficult to understand the structure-function correlation of cluster catalysts. There are still many things to be revealed on such complicated structures of metal clusters and their intermetallic interactions with solid supports.¹³ However, conventional structural analyses based on spectroscopy or diffraction could not determine the exact structure because they merely provide the average structure.

In order to experimentally investigate the fluctuating clusters, both a time resolution and atomic-level spatial resolution are necessary. Recent advances in transmission electron microscopes and scanning tunneling microscopes enabled recording the behavior with a sub-angstrom resolution in real time that has been used not only for the observation of a

molecular conformational change,¹⁴ reaction,¹⁵ solid surface reconstruction,¹⁶ metal cluster diffusion,¹⁷ metal cluster growth to nanoparticles,^{18,19} their coalescence^{20,21} or dissociations into atoms,²² but also for the visualization of cluster fluctuations.^{23,24} In our previous report on the atom-precise chemical synthesis of Pt₅–Pt₁₂, we witnessed constantly fluctuating movement of atoms in each cluster.²⁵ A detailed analysis of the movement may provide the physicochemical principles working between each metal atom that is essential for understanding the nature of the metal clusters. We now show the structural changes in the clusters composed of four atoms along with the analysis of the interaction between atoms.

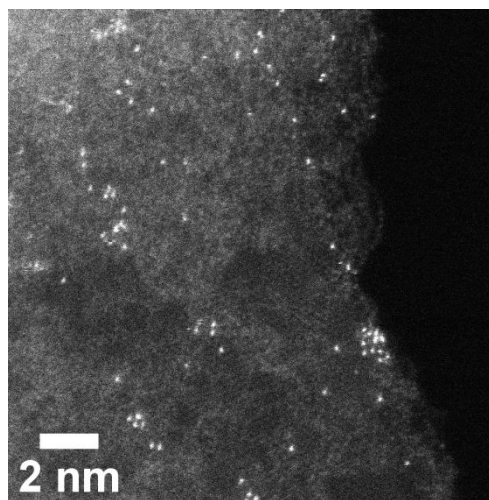


Fig. 1 Typical HAADF-STEM images (80 kV) of platinum clusters and atoms on graphene sheet prepared by arc-plasma deposition method operated with 360 μF condenser capacitance.

Graphene nanoplates dispersed in a methanol solvent were cast on commercially available thin holey carbon film coated Cu grid for TEM observation. Onto this graphene-modified grid, a small amount of Pt atoms was scattered by arc-plasma deposition (APD) method as described in ESI†.^{26,27} Upon one shot of the arc-plasma discharge (100 V, 360 μF), the resulting dispersion of

^a Laboratory for Chemistry and Life Science (CLS), Institute of Innovative Research (IIR), Tokyo Institute of Technology, Yokohama 226-8503, Japan.

E-mail: yamamoto@res.titech.ac.jp, timaoka@res.titech.ac.jp

^b ERATO-JST Yamamoto Atom Hybrid Project, Tokyo Institute of Technology, Yokohama 226-8503, Japan.

^c PRESTO-JST, Kawaguchi, 332-0012, Japan.

† Electronic Supplementary Information (ESI) available: [Experimental details and supporting data including STEM image, STEM video and DFT calculation results]. See DOI: 10.1039/x0xx00000x

Pt atoms on the graphene was suitable for the observation of tiny Pt clusters (Fig. 1). More shots or higher condenser capacities (720 μF) afforded larger clusters with a very narrow cluster-to-cluster distance (Fig. S1, ESI[†]), which is unsuitable for the observation of discrete clusters. Based on the initial investigation, we optimized the APD condition at 100 V and 360 μF for the following HAADF-STEM observations.

There were many tiny clusters of which size ranged from a single atom to ca. 10 atoms on a flat graphene sheet. Each cluster exhibited fluctuation during the observation of Cs-corrected STEM (JEM-ARM200F, 80 kV) with the 26 pA probe current scanned over a square area with 3.5 nm sides. Although most of the clusters are in the steady-state under the beam irradiation, a higher beam current or acceleration voltage tends to induce the irreversible degradations as previously reported.²² A narrower scan area with a fewer number of sampling pixels increases the time resolution thus allowing the real-time observation of the cluster fluctuation at a rate of 0.2 seconds per frame. Fig. 2a shows the snapshot images, and the original video (Fig. S2a, ESI[†]) exhibits the typical real-time behaviour of Pt₄ under the observed conditions.

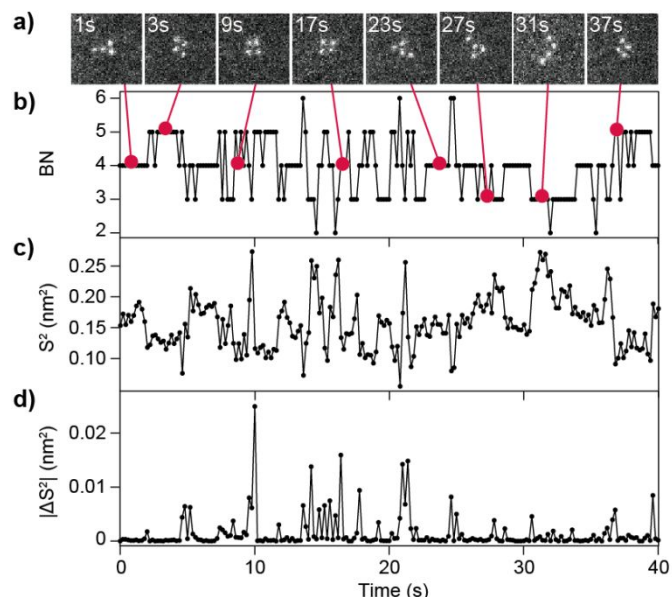


Fig. 2 Fluctuation of a Pt₄ cluster under the HAADF-STEM observation. (A) Snapshot images of the cluster. The box size is 2 nm \times 2 nm. (B) Transitions of a number of bonds (<math>< 0.30\text{ nm}</math>) in the cluster, (C) Transitions of the square radius of gyration (S^2), (D) Difference of the square radius of gyration $|\Delta S^2|$ as the indicator of cluster isomerization.

The video analysis of Pt₄ elucidated the continuous isomerizations of the cluster in which platinum atoms irregularly moved. According to the previously reported structural analysis of the W₇O_x clusters²² or rhenium clusters²⁸ on graphene successfully provided the realistic interatomic distances by STEM, thus we also assumed that the observation direction of the STEM is perpendicular to the surface of graphene. Based on the idea, extractions of four atomic coordinates on the XY plane horizontal to the graphene surface are possible from each frame of the STEM images. In some images, only three atoms were visible where the brightness of

one atom doubled in some images. Because the brightness of the HAADF-STEM is proportional to the number of atoms according to the Z contrast, it is reasonable to understand that two atoms are overlapping in the upright position in this case.²⁹ Although the Z coordinate is not available by the STEM, we assumed that the Z coordinate of all atoms is 0 for the convenience of analysis. Details about this validity will be discussed later, however, in conclusion, most of the platinum atoms with a few exceptions are located on the same plane, thus allowing the qualitative structural analysis.

From a continuous observation of 40 seconds, a total of 200 straight time-lapse images (5 still images per second) were available to collect the coordinates of four atoms using ImageJ software as described in ESI[†].³⁰ A histogram of all the interatomic distances (Fig. 3) from the six pairs between four atoms in each frame provided the structural information. The average distance between all interatomic pairs was 0.3 nm, but 0.25–0.28 nm was the most common, similar to the interatomic distance of the bulk fcc Pt metal (0.277 nm). On the other hand, the count was not negligible for the distances longer than 0.32 nm. These longer distances are not the first proximity but the second or further proximity. Note that other Pt₄ clusters found in different views also exhibited similar behavior (Fig. S2b). However, another particle tended to adopt different structural behavior such as preferential upright stacking of atoms (Fig. S2c, ESI[†]), probably due to the structural defect of graphene. This indicates that the structure of Pt₄ is susceptible to the surface of a support.

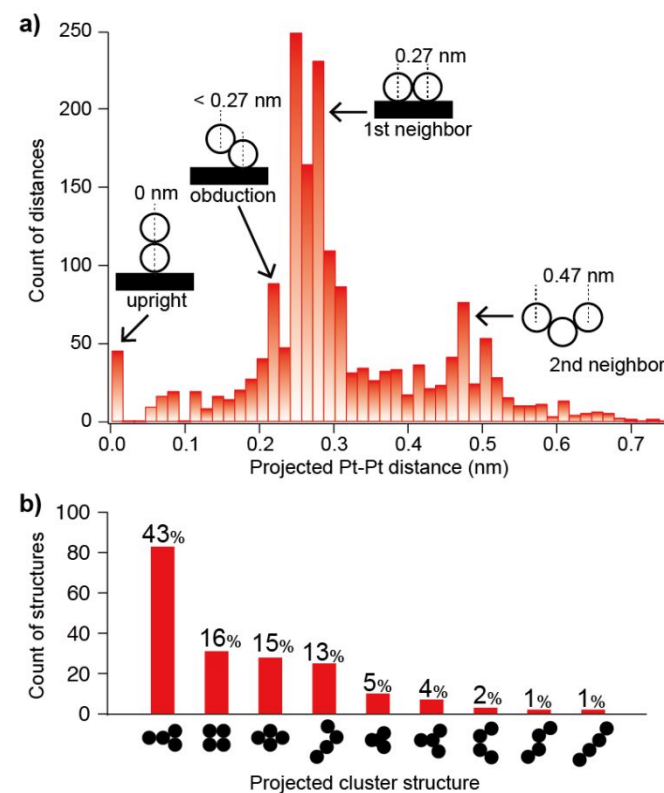


Fig. 3 (A) A histogram of the projected Pt-Pt distance in the HAADF-STEM images of Pt₄. (B) A histogram of the observed Pt₄ structures.

Previously reported theoretical calculations indicated the short Pt-Pt distance (0.23 - 0.26 nm) in the Pt₄ clusters with linear (1D), planar (2D) and spherical (3D) shapes in a vacuum.³¹ The present result qualitatively agrees with the idea. However, impractically short interatomic distances (0.00-0.23 nm) also exist in the histogram. When we assume the 2-dimensional cluster structures containing such a very close distance (< 0.23 nm), the corresponding DFT calculation indicated very high formation energies (>5 eV) which is thermodynamically unfavourable. This result suggests that it is reasonable to consider some of the Pt atoms locating in an upright position or obducting on another Pt atom.

When the interatomic distance shorter than 0.30 nm was defined as the direct Pt-Pt bond, BN=4 is the most frequent structure (Fig. 3b) as indicated by the histogram of the bond number (BN). The BN=4 cluster correspond to a square cluster (9 s or 17 s in Fig. 2a) or a triangle cluster with one additional on-top atom (1 s or 23 s in Fig. 2a). On the other hand, BN = 5 and BN = 3 corresponds to a rhomboid structure and open structures such as I, L or C alphabetical letter shapes, respectively. During the observation, the BN randomly walked back and forth between 5 and 3 (Fig. 2b). Especially, the triangle with one additional on-top atom, and square and rhomboid structures were commonly observed (Fig. 3b).

This observation does not quantitatively agree with the calculation result that the tetrahedral Pt₄ (BN=6) is the most stable structure when it was neutral or monocationic species (Fig. S3a, S3c, ESI[†]). There are several explanation for the disagreement. Firstly, diamonds (BN=5) and other BN = 4 clusters are entropically favourable due to the larger number of possible structures. Secondly, the lower dimensional structures (CN = 3, 4, 5) could be more stabilized by the interaction with graphene. However, the energy of each BN=4 cluster structures is about 0.2-0.7 eV higher than that of tetrahedron (BN=6) in vacuum, which seems insufficient for the justification of the observation. A possible explanation is that the Pt₄ was mono-anion. Our DFT calculation (Fig. S3b, ESI[†]) and previous study³² suggested that two-dimensional structures are much more stabilized when the cluster was mono-anion.

Is the fluctuation entirely random phenomena similar to that of the thermal isomerization of a molecule? To understand the mechanism, the duration time between every isomerization were determined from the time course. The square radius of gyration (S^2) calculated from the atomic coordination structure (ESI[†]) exhibited a random walking fluctuation behavior (Fig. 2c). Here, the moment of isomerization was defined as the point at which the difference in S^2 between each sampling frame ($|\Delta S^2|$) is greater than the threshold value of 0.0003 nm². This definition was determined to show good agreement with the moment of structural isomerization with visually recognizable topology change. The cumulative probability distribution of the lifetime (Fig. 4) agrees with the theory of exponential distribution, which means the time interval of events following random Poisson process. This fact suggests that the isomerizations are entirely a random and memoryless phenomena. Application to a first-order reaction model allows us to estimate the reaction constant of the isomerization as 4.2

s⁻¹. This random characteristic is similarly observed in other fields of view. However, the validity of the reaction constant should not be overstated. For example, the other clusters shown as Figs. S2b and S2c provided 2.6 s⁻¹ and 3.7 s⁻¹, respectively (Figs. S4a and S4b). Further assessment with a lot of experimental data is required to clarify the experimental errors and the difference in intrinsic properties depending on the locations.

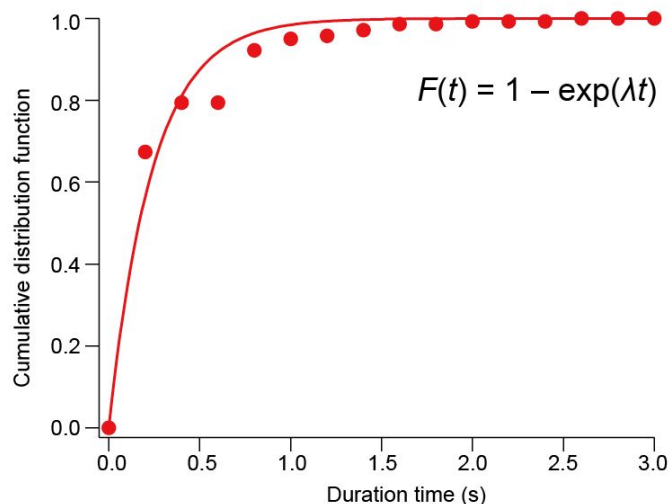


Fig. 4. The cumulative probability distribution of the lifetime during the structural isomerizations (circle). The horizontal axis means the duration time of each cluster structure. The moments of structural transitions were defined as $|\Delta S^2| > 0.0003$ nm² where significant changes in S^2 were found. The solid line is the regression analysis result using the equation shown in the figure ($\lambda = 4.2$ s⁻¹).

In summary, realtime observation of a four-platinum-atom cluster at the atomic resolution experimentally revealed the several stable structures and their isomerization kinetics being first-order rate. Although we should take location dependence of the fluxionality on the support containing substantial defect points, an accurate reaction temperature, and the influence of instantaneous ionization by electron beam irradiation into account for a more quantitative understanding, this method would open a new avenue for the experimental study of the fluctuating clusters.

This study was supported in part by JST ERATO Grant Number JPMJER1503, Japan (K.Y.), JST PRESTO Grant Number JPMJPR1511, Japan (T.I.), JSPS KAKENHI Grant Nos. JP 15H05757 (K.Y.), JP 16H04115 (T.I.) and the Cooperative Research Program of "Network Joint Research Center for Materials and Devices".

Conflicts of interest

There are no conflicts to declare.

Notes and references

- 1 L. Liu and A. Corma, *Chem. Rev.*, 2018, **118**, 4981–5079.
- 2 Y.-X. Zhao, Z.-Y. Li, Y. Yang and S.-G. He, *Acc. Chem. Res.*,

- 2018, **51**, 2603–2610.
- 3 E. C. Tyo and S. Vajda, *Nature Nanotech.*, 2015, **10**, 577–588.
- 4 C. Deraedt and D. Astruc, *Acc. Chem. Res.*, 2014, **47**, 494–503.
- 5 K. Yamamoto, T. Imaoka, W.-J. Chun, O. Enoki, H. Katoh, M. Takenaga and A. Sonoi, *Nature Chem.*, 2009, **1**, 397–402.
- 6 T. Imaoka, H. Kitazawa, W.-J. Chun and K. Yamamoto, *Angew. Chem. Int. Ed.*, 2015, **127**, 9948–9953.
- 7 M. Huda, K. Minamisawa, T. Tsukamoto, M. Tanabe and K. Yamamoto, *Angew. Chem. Int. Ed.*, 2018, **343**, 393.
- 8 H. Zhai and A. N. Alexandrova, *ACS Catal.*, 2017, **7**, 1905–1911.
- 9 V. Fung and D.-E. Jiang, *J. Phys. Chem. C*, 2017, **121**, 10796–10802.
- 10 M. R. Fagiani, X. Song, P. Petkov, S. Debnath, S. Gewinner, W. Schöllkopf, T. Heine, A. Fielicke and K. R. Asmis, *Angew. Chem. Int. Ed. Engl.*, 2017, **56**, 501–504.
- 11 A. V. Pisliakov, J. Cao, S. C. L. Kamerlin and A. Warshel, *Proc. Natl. Acad. Sci. U.S.A.*, 2009, **106**, 17359–17364.
- 12 M. Karplus, *Proc. Natl. Acad. Sci. U.S.A.*, 2010, **107**, E71–author reply E72.
- 13 A. Bruix, J. A. Rodríguez, P. J. Ramírez, S. D. Senanayake, J. Evans, J. B. Park, D. Stacchiola, P. Liu, J. Hrbek and F. Illas, *J. Am. Chem. Soc.*, 2012, **134**, 8968–8974.
- 14 E. Nakamura, *Acc. Chem. Res.*, 2017, **50**, 1281–1292.
- 15 S. Okada, S. Kowashi, L. Schweighauser, K. Yamanouchi, K. Harano and E. Nakamura, *J. Am. Chem. Soc.*, 2017, **139**, 18281–18287.
- 16 N. Kamiuchi, K. Sun, R. Aso, M. Tane, T. Tamaoka, H. Yoshida and S. Takeda, *Nature Commun.*, 2018, **9**, 2060.
- 17 B. A. J. Lechner, F. Knoller, A. Bourgund, U. Heiz and F. Esch, *J. Phys. Chem. C*, 2018, **122**, 22569–22576.
- 18 H.-G. Liao, D. Zherebetsky, H. Xin, C. Czarnik, P. Ercius, H. Elmlund, M. Pan, L.-W. Wang and H. Zheng, *Science*, 2014, **345**, 916–919.
- 19 Z. Zeng, W. Zheng and H. Zheng, *Acc. Chem. Res.*, 2017, **50**, 1808–1817.
- 20 J. M. Yuk, M. Jeong, S. Y. Kim, H. K. Seo, J. Kim and J. Y. Lee, *Chem. Commun.*, 2013, **49**, 11479–11481.
- 21 T. J. Woehl, C. Park, J. E. Evans, I. Arslan, W. D. Ristenpart and N. D. Browning, *Nano Lett.*, 2014, **14**, 373–378.
- 22 H. Yasumatsu, T. Tohei and Y. Ikuhara, *J. Phys. Chem. C*, 2014, **118**, 1706–1711.
- 23 S. Bals, S. Van Aert, C. P. Romero, K. Lauwaet, M. J. Van Bael, B. Schoeters, B. Partoens, E. Yücelen, P. Lievens and G. Van Tendeloo, *Nature Commun.*, 2012, **3**, 897.
- 24 Z. W. Wang and R. E. Palmer, *Nanoscale*, 2012, **4**, 4947–4.
- 25 T. Imaoka, Y. Akanuma, N. Haruta, S. Tsuchiya, K. Ishihara, T. Okayasu, W.-J. Chun, M. Takahashi and K. Yamamoto, *Nature Commun.*, 2017, **8**, 43.
- 26 S. Hinokuma, S. Misumi, H. Yoshida and M. Machida, *Catal. Sci. Technol.*, 2015, **5**, 4249–4257.
- 27 Y. Agawa, S. Endo, M. Matsuura and Y. Ishii, *ECS Trans.*, 2013, **50**, 1271–1276.
- 28 O. Miramontes, F. Bonafé, U. Santiago, E. Larios-Rodríguez, J. J. Velázquez-Salazar, M. M. Mariscal and M. J. Yacamán, *Phys. Chem. Chem. Phys.*, 2015, **17**, 7898–7906.
- 29 A. De Backer, G. T. Martínez, A. Rosenauer and S. Van Aert, *Ultramicroscopy*, 2013, **134**, 23–33.
- 30 C. A. Schneider, W. S. Rasband and K. W. Eliceiri, *Nature Methods*, 2012, **9**, 671–675.
- 31 L. Xiao and L. Wang, *J. Phys. Chem. A*, 2004, **108**, 8605–8614.
- 32 A. S. Chaves, G. G. Rondina, M. J. Piotrowski, P. Tereshchuk and J. L. F. Da Silva, *J. Phys. Chem. A*, 2014, **118**, 10813–10821.